



Published in final edited form as:

Nature. 2015 June 18; 522(7556): 315–320. doi:10.1038/nature14451.

A novel multiple-stage antimalarial agent that inhibits protein synthesis

A full list of authors and affiliations appears at the end of the article.

Summary

There is an urgent need for new drugs to treat malaria, with broad therapeutic potential and novel modes of action, to widen the scope of treatment and to overcome emerging drug resistance. We describe the discovery of DDD107498, a compound with a potent and novel spectrum of antimalarial activity against multiple life-cycle stages of the parasite, with good pharmacokinetic properties, and an acceptable safety profile. DDD107498 demonstrates potential to address a variety of clinical needs, including single dose treatment, transmission blocking and chemoprotection. DDD107498 was developed from a screening programme against blood stage malaria parasites; its molecular target has been identified as translation elongation factor 2 (eEF2), which is responsible for the GTP-dependent translocation of the ribosome along mRNA, and is essential for protein synthesis. This discovery of eEF2 as a viable antimalarial drug target opens up new possibilities for drug discovery.

Introduction

The WHO estimates there were approximately 200 million clinical cases and 584,000 deaths from malaria in 2013, predominantly amongst children and pregnant women in sub-Saharan Africa¹. The malaria parasite has developed resistance to many of the current drugs, including emerging resistance to the core artemisinin component of artemisinin-based combination therapies that comprise current first-line therapies². To support the current treatment and eradication agenda³, there are a number of requirements for new antimalarials: novel modes of action with no cross-resistance to current drugs; single dose cures; activity against both the asexual blood stages that cause disease and gametocytes responsible for transmission; compounds which prevent infection (chemoprotective agents); and compounds which clear *P. vivax* hypnozoites from the liver (anti-relapse agents)⁴.

Discovery of a novel antimalarial

A phenotypic screen of the Dundee protein kinase scaffold library⁵ (then 4731 compounds) was performed against the blood stage of the multi-drug sensitive *P. falciparum* 3D7 strain.

Reprints and permissions information is available at npg.nature.com/reprintsandpermissions.

Correspondence and requests for materials should be addressed to I.H.G (i.h.gilbert@dundee.ac.uk) or K.D.R (k.read@dundee.ac.uk).

Author Contributions The author contributions are detailed in the Supplementary Information.

Author Information A patent relating to this work has been filed (PCT/GB2009/002084). Koen Dechering and Robert Sauerwein have shares in TropIQ Health Sciences.

Supplementary Information is linked to the online version of the paper at www.nature.com/nature.

A compound series from this screen, based on a 2,6-disubstituted quinoline-4-carboxamide scaffold, had sub-micromolar potency against the parasites, but suffered from poor physicochemical properties. Chemical optimisation (Fig. 1 and Extended Data Fig. 1) led to DDD107498 with improved physicochemical properties (Supplementary Methods Tables S1 and S2) and a 100-fold increase in potency. The key stages involved were: replacing the bromine with a fluorine atom to reduce molecular weight and lipophilicity; replacing the 3-pyridyl substituent with an ethylpyrrolidine group, and addition of a morpholine group via a methylene spacer. Initial cost of goods estimates together with likely human dose projections suggest a low cost (approximately US\$1 per treatment), which is important, given most of the patient population is living in poverty.

Blood-stage activity and developability

DDD107498 showed excellent activity against 3D7 parasites: $EC_{50} = 1.0$ nM (95% Confidence Interval (CI) 0.8-1.2 nM); $EC_{90} = 2.4$ nM (95% CI 2.0-2.9 nM); $EC_{99} = 5.9$ nM (95% CI 4.5-7.6 nM), (n=39). It was also almost equally active against a number of drug-resistant strains (Extended Data Fig. 2a)⁶. Furthermore, DDD107498 was more potent than artesunate in *ex vivo* assays against a range of clinical isolates of both *P. falciparum* (median $EC_{50} = 0.81$ [Range 0.29-3.29] nM, n=44) and *P. vivax* (median $EC_{50} = 0.51$ [Range 0.25-1.39] nM, n=28), collected from patients with malaria from Southern Papua, Indonesia, a region where high-grade multidrug-resistant malaria is endemic for both species (Extended Data Fig. 2b)^{7,8}. In contrast the compound was not toxic to human cells (MRC5 and Hep-G2 cells) at much higher concentrations (> 20,000 fold selectivity, Extended Data Fig. 2c).

DDD107498 showed good drug-like properties: metabolic stability when incubated with hepatic microsomes or hepatocytes from several species; good solubility in a range of different media; and low protein binding (Supplementary Methods, Tables S1 and S2). DDD107498 displayed excellent pharmacokinetic properties in preclinical species, including good oral bioavailability, an important pre-requisite for use in resource-poor settings, and long plasma half-life, important for single dose treatment and chemoprotection (Extended Data Table 1a).

DDD107498 was very active in several mouse models of malaria, with comparable or greater efficacy than current antimalarials (Extended Data Table 1b). DDD107498 had an ED_{90} (90% reduction in parasitaemia) of 0.57 mg/kg after a single oral dose in mice infected with the rodent parasite *P. berghei*. Efficacy was also tested in NOD-*scid* IL-2R₀*null* mice engrafted with human erythrocytes and infected with *P. falciparum* strain 3D7^{0087/N9} (Fig. 2a)⁹. When dosed orally daily for 4 days, the ED_{90} on day 7 after infection was 0.95 mg/kg per day. Blood sampling from the infected SCID mice suggested a minimum parasitocidal concentration (MPC) for DDD107498 of 10-13 ng/mL for asexual blood stage infections.

The effects of DDD107498 on circulating parasites in the SCID mouse model could be observed in one replication cycle (48 h) and led to trophozoites with condensed cytoplasm (Extended Data Fig. 3). Stage specificity studies using synchronized cultures showed that at a concentration of 4nM for 24 h, DDD107498 led to: (1) from the ring stage, formation of abnormal trophozoites; (2) from the trophozoite stage, prevention of schizont formation with a 50% reduction in parasites, indicative of cidal activity; (3) from the schizont stage,

prevention of ring formation with a 98% reduction in parasites, indicative of cidal activity (Extended Data Fig. 3b,c).

DDD107498 showed a similar parasite killing profile both *in vitro* (Fig. 2b,c) and *in vivo* (Fig. 2a) which is supportive of a common mode of action in cellular and animal models of disease. Using a Parasite Reduction Rate (PRR) assay¹⁰ there was a lag of about 24-48 h during which time the effects of the compounds were reversible following wash-out. Rapid killing occurred after parasites had been exposed to DDD107498 for more than 48 h (Figs. 2b,c).

All these experiments suggest for the blood stage form that treatment with DDD107498 prevented development of trophozoites and schizonts and at least in the case of schizonts caused rapid killing. Any ring stage parasites only developed as far as abnormal trophozoites, which appeared to survive for about 48 h under drug pressure, but then were killed.

In safety studies, DDD107498 showed no significant inhibition of any of the major human cytochrome P450 (CYP) isoforms and CYP450 induction risk was low (Supplementary Methods, Table S3), indicating a low risk of clinical drug-drug interactions. DDD107498 is non-mutagenic and has very weak inhibitory potencies on I_{Kr} (hERG) and other ion channels indicating a very low risk for adverse cardiovascular activity. However, given its potency, long half-life observed in preclinical species, and safety margins from a rat 7-day toxicology study, DDD107498 has potential for both single dose treatment and once weekly chemoprotection¹¹.

Activity against other life-cycle stages

Activity against intra-hepatocytic parasites (liver schizont stages)—This is the first stage of human infection after injection of sporozoites by anopheline mosquitoes, where the parasites invade and multiply in the liver. Compounds active against this stage have potential for use in chemoprotection. DDD107498 showed an EC₅₀ ~ 1 nM against the liver schizont forms of *P. berghei* and *P. yoelii*¹². DDD107498 was active when dosed for only 2 h during the initial infection (hepatocyte invasion) of the liver cells (Fig. 3). In contrast, atovaquone (clinically used for chemoprotection in combination with proguanil) had a significantly reduced activity during this period (EC₅₀ ~ 106 nM versus 0.3 nM for continuous treatment). Further, DDD107498 showed equivalent potency against the *P. berghei* liver stage when dosed for a short period of time after initial infection had been established (Fig. 3). This suggests that intermittent treatment may be sufficient for chemoprotection. To assess chemoprotective potential *in vivo*, mice were treated with DDD107498 2 h before being infected with luciferase-expressing *P. berghei* sporozoites (Extended Data Fig. 4). At a dose of 3 mg/kg, DDD107498 was fully curative with no sign of parasitaemia after 30 days. Thus, DDD107498 demonstrates potent chemoprotection using *in vitro* and *in vivo* models, where blood sampling from the mice during the experiment suggests a MPC of 15-20 ng/mL.

Transmission Blocking—The parasite erythrocytic form differentiates into the asymptomatic male and female gametocytes (stages I-V) within the human host. Mature

stage V gametocytes are infective to mosquitoes, but are not eliminated by the majority of current antimalarial agents, and remain circulating in the human bloodstream for up to 3 weeks, long after the disappearance of clinical symptoms of malaria^{13,14}. After ingestion by the mosquito, gametocytes differentiate into gametes. DDD107498 potently inhibited both male and female gamete formation from the gametocyte stage at similar concentrations (1.8nM [95% CI 1.6-2.1nM] and 1.2nM [95% CI 0.8-1.6nM] respectively, Extended Data Fig. 5), indicating that it is an extremely potent inhibitor of the functional viability of both male and female mature gametocytes¹⁵. In line with this, DDD107498 blocked transmission as determined by the Standard Membrane Feeding Assay (SMFA). In this assay, parasite cultures containing *P. falciparum* stage V gametocytes were exposed to compound for 24 h prior to mosquito feeding. DDD107498 blocked subsequent oocyst development in the mosquito (measured after 7 days) with an EC₅₀ of 1.8 nM. At a baseline oocyst intensity of 27 oocysts per mosquito in the DMSO controls, prevalence of infection was inhibited with an EC₅₀ of 3.7 nM as measured by the number of infected mosquitoes. Repeating the SMFA in which DDD107498 was added at the moment of mosquito feeding gave an EC₅₀ of 10 nM, indicating potent activity against the parasite sexual stages that develop in the mosquito midgut (Extended Data Fig. 5)¹⁶.

A *P. berghei* mouse-to-mouse^{17,18} model was additionally used to examine transmission-blockade. Mice were infected with *P. berghei* (PbGFPCON507)¹⁹, and then treated orally with compound 24 h before mosquitoes took a direct blood meal¹⁷. After a 3 mg/kg dose of DDD107498, a 90.7% reduction in infected mosquitoes and a 98.8% reduction in oocysts per midgut was observed at day 10 in comparison with mosquitoes fed on untreated mice (Extended Data Fig. 6). A corresponding reduction in sporozoite intensity and prevalence was observed (93.8% and 88.6% respectively). Mosquitoes previously fed on infected, drug treated mice were allowed to feed on uninfected mice¹⁷. Over multiple mosquito biting rates, a 89.5% (95% CIs 71.4-100) reduction in the number of mice that developed blood stage infection was observed in comparison with mice bitten by mosquitoes that had fed on non drug-treated infected mice. The overall effectiveness of an intervention over a round of transmission (from mouse to mosquito to mouse) can be quantified by estimating its ability to reduce the basic reproductive number (R_0). This has been termed the “effect size” of an intervention. By fitting data from the mouse-to-mouse assay to a chain binomial model we can estimate the effect size of the intervention¹⁷, assessing the ability of DDD107498 usage to reduce the basic reproductive number R_0 (assuming 100% coverage). Our results estimate an effect size of 90.5% (95% CIs 78.3-94.2), suggesting that DDD107498 is capable of acting as a potent transmission-blocking drug over multiple transmission settings within a field context¹⁸. The combination of these key *in vitro* and *in vivo* assays demonstrate the very strong potential of DDD107498 for blocking transmission; importantly, the required doses are likely to be similar to those required for treatment of blood-stage malaria.

DDD107498 targets *PfeEF2*

To determine the molecular target for DDD107498, asexual blood stage *P. falciparum* were cultured in the presence of DDD107498 at $5 \times EC_{50}$, until parasites became resistant (Extended Data Table 2)²⁰. Resistance was obtained in the 3D7 (drug sensitive) and 7G8 and Dd2 (multi-drug resistant) strains, with minimum inocula of 10^7 , 10^7 and 10^6

respectively. Genomic DNA was extracted from resistant lines and whole genome sequencing of 10 drug-resistant lines identified shared mutations in one gene, which were not present in the parental lines: Pf3D7_1451100 (Supplementary Data 1). This gene encodes *P. falciparum* translation elongation factor 2 (*PfeEF2*). Three lines had two single nucleotide polymorphisms (SNPs) in *PfeEF2*, with a mixture of wildtype (WT) and mutant reads at each position (Supplementary Data 2), suggesting that these lines were mixtures of two clones, each with independent mutations in *PfeEF2*. SNPs were confirmed by Sanger sequencing and nine validated mutations in *PfeEF2* clustered in three regions of the encoded protein. The fact that resistance to DDD107498 can be associated with multiple independent mutations is in keeping with observations from both artemisinin and compounds in development²¹⁻²³. In two cases identical SNPs were identified in two independent lines, indicating mutations in functionally significant residues that were acquired independently in separate selection experiments.

eEF2 is one of several essential elongation factors required in eukaryotic protein synthesis, by mediating GTP-dependent translocation of the ribosome along mRNA (Fig. 4a)²⁴. Yeast eEF2 is the target of the antifungal compound sordarin^{25,26}. Sordarin is selective for the *Saccharomyces cerevisiae* eEF2 over mammalian eEF2 *in vitro*, demonstrating that although protein synthesis in eukaryotes is conserved, it is possible to obtain selective inhibitors, despite the relatively high homology (67.2% identity) between the yeast and human eEF2 (Extended Data Fig. 7)^{25,27}. In keeping with the potential for selectivity, DDD107498 is not toxic to mammalian cells (Extended Data Fig 2c). The *PfeEF2* mutations associated with resistance mapped to several areas on the surface of a homology model of the protein (based on the *apo* structure of *S. cerevisiae* eEF2²⁸), with the mutations giving the highest degree of resistance clustering together (Fig. 4b). A DDD107498 binding pocket could not be elucidated through these modeling studies.

We confirmed that brief pre-incubation with DDD107498 specifically inhibited *P. falciparum* protein synthesis, by measuring short-term incorporation of [³⁵S]-Met/Cys in WT and DDD107498-resistant 3D7 *P. falciparum* parasites (Fig. 4d)²¹. Cycloheximide (a protein synthesis inhibitor) and DDD107498 both prevented [³⁵S]-Met/Cys incorporation into WT *P. falciparum* 3D7, whereas actinomycin D (an inhibitor of RNA transcription) had no effect. Notably, DDD107498 was 100-fold less effective in DDD107498-resistant 3D7 compared to WT parasites, whereas cycloheximide prevented [³⁵S]-Met/Cys incorporation equally in resistant and WT lines. DDD107498 and cycloheximide had minimal effects on DNA/RNA biosynthesis in both sensitive and drug-resistant parasites (measured by incorporation of [³H]-hypoxanthine), demonstrating specificity. In contrast actinomycin D caused a significant dose-dependent reduction in [³H]-incorporation.

To confirm that *PfeEF2* is the target for DDD107498, we integrated transgenes expressing either WT *PfeEF2* or resistance-associated alleles of *PfeEF2* (Y186N, observed in mutant Dd2 and P754S, observed in mutant 3D7) using attPxattB integrase-mediated recombination^{21,29}. These transfectants also express endogenous *PfeEF2*. Imaging of GFP-fusions of *PfeEF2* showed cytoplasmic localisation (Fig. 4c), indicating that DDD107498 inhibits protein synthesis in the cytoplasm as opposed to the apicoplast³⁰, the site of action of tetracycline and azithromycin.

Dose-response assays with DDD107498 showed a similar inhibition profile between *PfeEF2* transgene-expressing lines and the WT Dd2 strain, indicating that the endogenous WT-*PfeEF2* has a dominant effect in these experiments (Fig. 4e). This may be due to stable complex formation between the ribosome, WT-*PfeEF2* and DDD107498, resulting in ribosome stalling, which would explain why in mixed populations the WT-*PfeEF2* is dominant. For example in bacteria, fusidic acid binds to the complex between EF-G and the ribosome, preventing dissociation and blocking protein translation³¹.

To determine whether WT-*PfeEF2* was dominant in poisoning translation, we introduced episomal plasmids encoding WT or Y186N mutant *PfeEF2* into the resistant *PfeEF2* Y186N line (Fig. 4f). Plasmid-borne *PfeEF2*-Y186N had no effect on sensitivity to DDD107498 ($EC_{50} \sim 3100$ nM), whereas WT-*PfeEF2* restored sensitivity ($EC_{50} = 2$ nM). This demonstrated a dominant effect of WT-*PfeEF2* on parasite susceptibility and confirmed that *PfeEF2* is the primary molecular target of the compound. We note that the shallow slope observed for the WT-*PfeEF2* transfected line is likely a result of heterogeneous episomal plasmid copy number seen with episomally transformed parasite lines²⁹. Structural studies will be required to define precisely how DDD107498 interacts with eEF2 and the ribosome.

Resistance has been reported for all clinical antimalarials, including artemisinins². Whilst the correlation between the rate of resistance generation in laboratory and clinical settings for antimalarials is not fully understood, it is important to evaluate the risk of all new antimalarials in both preclinical and clinical studies. In our studies, the minimum inoculum for generating resistance to DDD107498 is within acceptable limits³². Furthermore, selected resistant Dd2 lines revealed impaired growth rates in the absence of drug pressure compared to WT-Dd2 (Extended Data Fig. 8); moreover the higher the resistance, the lower the growth fitness. Importantly genome sequences from 1685 clinical isolates of *P. falciparum* from 17 countries^{23,33} reveal a high degree of *PfeEF2* sequence conservation in the field. The sole non-synonymous SNP (T16S) identified was unique to West Africa (allele frequency of 0.002) and is in a *PfeEF2* domain distinct from mutations associated with *in vitro* resistance to DDD107498.

Conclusion

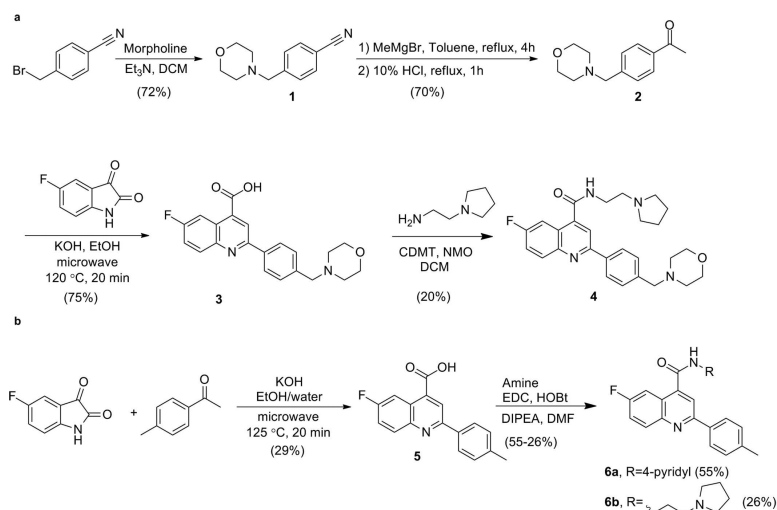
DDD107498 represents a promising prospect for development as an anti-malarial agent, with both a potent activity profile against multiple life-cycle stages (sub-10 nM), a novel mode of action and excellent drug-like properties. It has potential for single dose treatment, which has major implications for ensuring patient compliance and practical deployment. Its complementary activity on the sexual stages of the parasites has potential to reduce transmission and its action on the liver stage suggests a possible role in chemoprevention. Chemoprotection and transmission blocking properties are fundamental to the goal of elimination and eradication of malaria, for which the high potency and long half-life of DDD107498 are well suited.

Due to general concerns about the emergence of resistance, all antimalarials are developed as combination therapies, a strategy shown to improve efficacy and reduce the development of drug resistance. In terms of treatment of the erythrocytic stage, DDD107498 fulfils the

criteria as a long duration partner to complete the clearance of blood stage parasites¹¹. Therefore, it should be combined with a fast acting compound, ideally with a pharmacological duration of action as close to DDD107498 as possible. This would reduce the initial level of infection, with the prolonged activity of DDD107498 eliminating the remaining parasites¹¹.

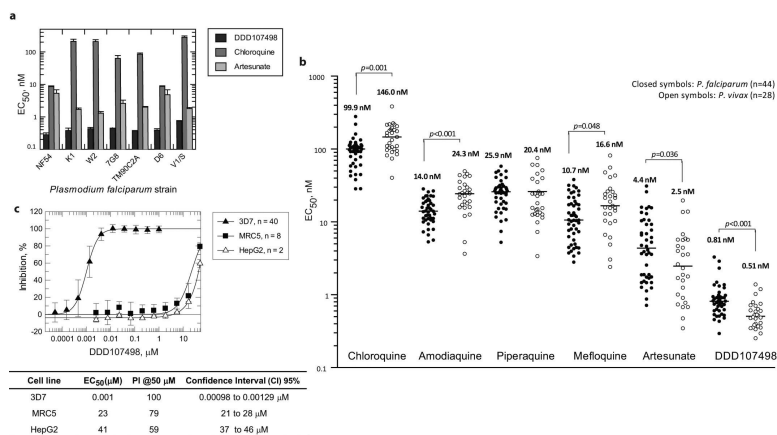
Inhibition of protein synthesis by DDD107498 through *PfeEF2*, which is expressed in multiple life cycle stages³⁴, provides mechanistic support for the observed broad-spectrum profile. This highlights *PfeEF2* as a novel drug target in malaria, and also implies that inhibition of protein synthesis is an effective intervention for achieving multi-stage activity in *Plasmodium*. DDD107498 has now been progressed into advanced nonclinical development, with the aim of entering into human clinical trials.

Extended Data



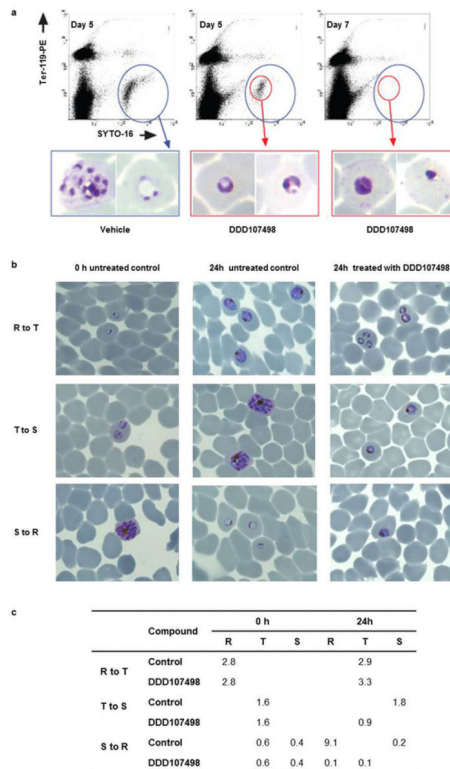
Extended Data Figure 1. Synthetic Methodology

a. Synthesis of DDD107498 (**4**). **b.** Synthesis of DDD102542 (**6a**) and DDD103679 (**6b**).



Extended Data Figure 2. In vitro Activity

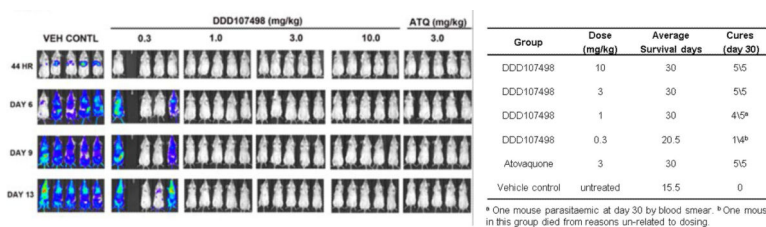
a. *In vitro* activity against a panel of resistant and sensitive strains of *P. falciparum*. Abbreviations: chloroquine (CQ), pyrimethamine (PYR), cycloguanil (CYC), quinine (QUI), sulfadoxine (SUL) and/or mefloquine (MFQ). Resistance as follows: K1 (CQ, SUL, PYR, CYC); W2 (CQ, SUL, PYR, CYC); 7G8 (CQ, PYR, CYC); TM90C2A (CQ, PYR, MFQ, CYC); D6 (MFQ); V1/S (CQ, SUL, PYR, CYC). Data are the means \pm s.d. of $n=3$ independent [^3H]hypoxanthine incorporation experiments (each run in duplicate). **b.** *Ex-vivo* activity against *P. falciparum* and *P. vivax* clinical isolates from Papua (Indonesia). **c.** Effect of DDD107498 on *P. falciparum* 3D7, HepG2 and MRC5 cells. Data are the means \pm s.d. of n reported independent experiments.



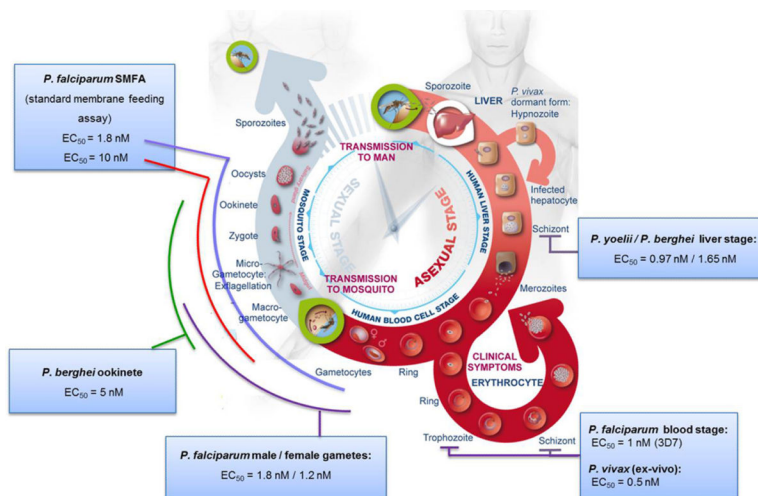
Extended Data Figure 3. Effect of DDD107498 on parasite morphology

a. Phenotype of *P. falciparum* in peripheral blood of NOD-*scid* IL-2R₀*null* mice engrafted with human erythrocytes. Blood samples were taken at day 5 and 7 of the assay (1 and 2 asexual cycles, respectively) after the start of treatment with vehicle or DDD107498 at day 3. The bidimensional flow cytometry plots measure the murine (Ter-119-PE⁺) and human (Ter-119-PE⁻) erythrocytes, and the presence of nucleic acids (infected SYTO-16⁺ events). The blue circles indicate the region of infected erythrocytes. Vehicle-treated mice showed a characteristic pattern of staining with SYTO-16³⁵, which correlated with the presence of healthy rings, trophozoites and schizonts in blood smears. Conversely, mice treated with DDD107498 at 50 mg/kg showed only trophozoites with condensed cytoplasm and some pyknotic cells at day 5 (red circle in flow cytometry plot and corresponding blood smears). By day 7, few infected erythrocytes were detected by flow cytometry and blood smears revealed parasites with a similar morphology to those at day 5. This suggests that trophozoites are the most sensitive population since the cycle is interrupted at this stage. The

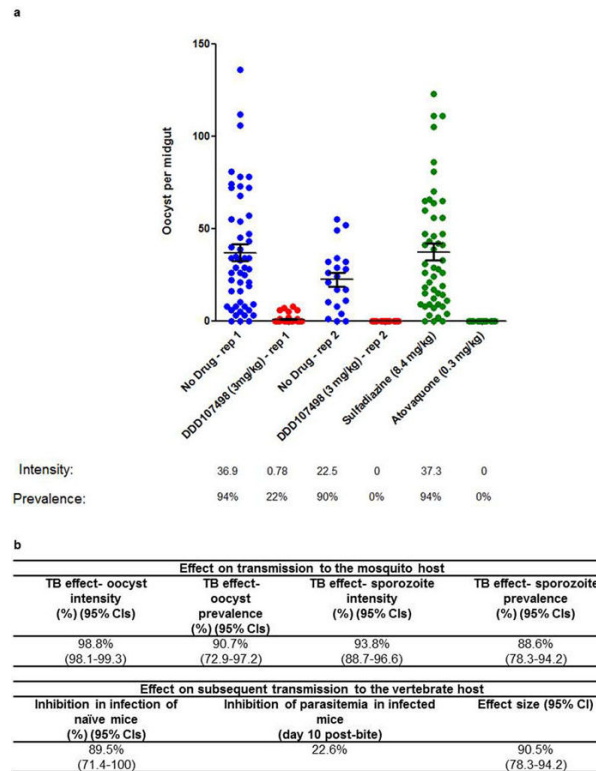
images displayed are taken from a mouse with high levels of parasitemia. At least 50 parasites were counted per sample screened in the microscope. Of these, 4 photos of representative parasite phenotype were selected to represent the morphology of the most prevalent phenotype. Thus, this is a qualitative assessment. **b.** Stage specificity assays using synchronised cultures. For morphological analysis of antimalarial drug action, thin blood smears were prepared, fixed and stained with Giemsa followed by examination with an upright microscope using an oil-immersion lens (100×). For parasitemia determination, a total number of 1000 red blood cells (corresponding to 5 microscopic fields) were counted. **R to T.** Abnormal trophozoites observed after 24h exposure of synchronized rings to DDD107498. **T to S.** Trophozoites do not develop into schizonts after 24h exposure to DDD107498. **S-R.** No ring stages are observed 24h after treatment of schizonts with DDD107498. **c.** Percentage parasitemia in the red blood cells. R = ring stage, T = trophozoite, S = schizont.



Extended Data Figure 4. Prophylactic activity of DDD107498 against sporozoite challenge *P. berghei* (luciferase) sporozoite *in vivo* mouse model of chemoprotection. A dose of 3mg/kg was fully protective. Data are the mean of n=5.



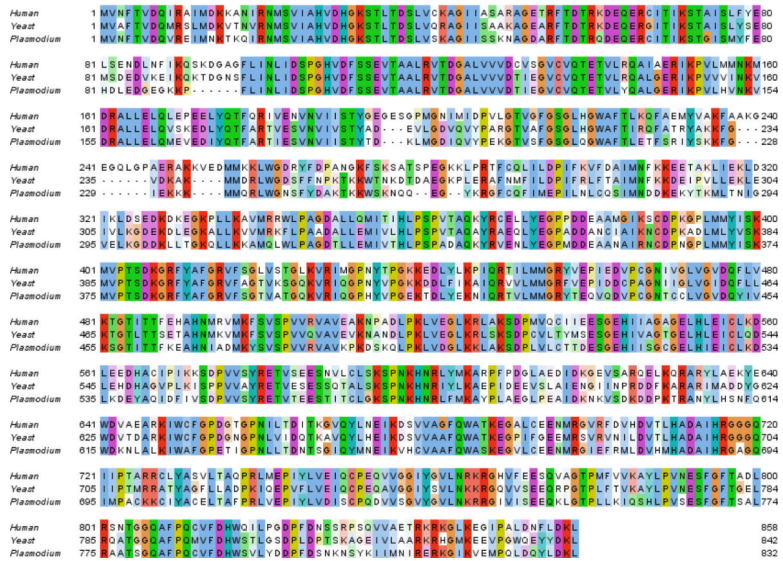
Extended Data Figure 5. DDD107498 *in vitro* activity on the different life cycle stages of *Plasmodium* spp. For comparator data with known antimalarials see Figure 5 in Delves *et al.*⁶ DDD107498 also showed potent activity *in vitro* against *P. berghei* ookinetes¹⁶, (5.0nM [CI 4.4-5.7nM]), confirming that if DDD107498 was taken up during a blood meal, it could continue to kill parasites within the mosquito.



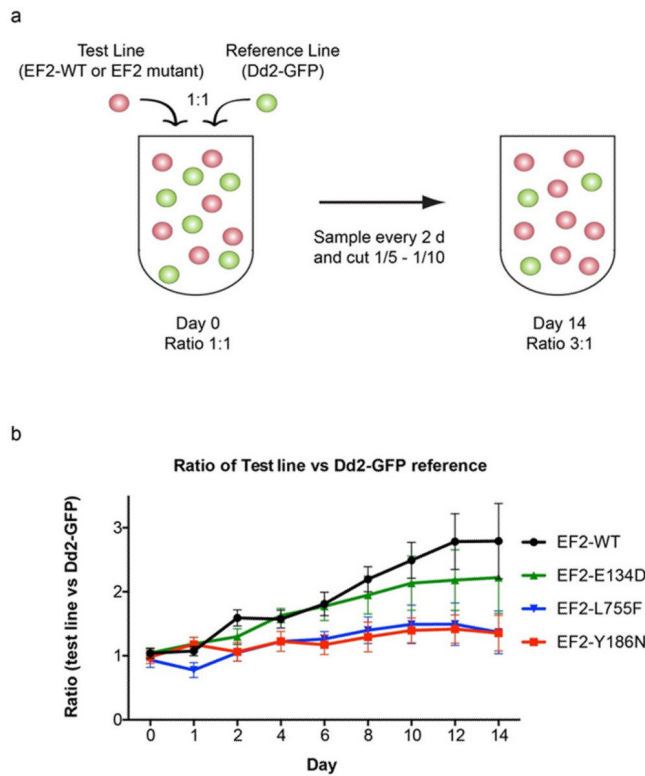
Extended Data Figure 6. *In vivo P. berghei* mouse-to-mouse assay

a. Impact of DDD107498 treatment on *in vivo* mosquito infection. Mice infected with *P. berghei* (PbGFPCON507 clone 1)¹⁹ were dosed orally with either DDD107489 at 3 mg/kg, atovaquone at 0.3 mg/kg, sulphadiazine at 8.4 mg/kg, or were not drug treated (negative control). After 24 h, populations of treated mice (n=5) were exposed to 500 female *A. stephensi* mosquitoes, and oocyst intensity and infection prevalence in the mosquito midgut was measured 10 days post-feeding. Individual data points represent the number of oocysts found in individual mosquitoes. Two replicates were performed. Sulphadiazine (8.4 mg/kg, *i.p.*) and atovaquone (0.3 mg/kg, *i.p.*) were used as negative and positive transmission-blocking drug controls, respectively. Horizontal bars indicate mean intensity of infection, whilst error bars indicate S.E.M. within individual mosquito populations. b. Impact of treatment with DDD107498 over a complete transmission cycle *in vivo*. Following drug treatment of infected mice and mosquito feeds, surviving potentially infectious mosquitoes were allowed to blood-feed on naïve mice at a range of transmission settings (biting rates of 2.5 and 10 bites per naïve mouse) to assess ability of drug treatment to reduce the number of new malarial cases post mosquito bite. Efficacy is expressed as: i) impact on the mosquito population – expressed as reduction in both oocyst and sporozoite intensity and prevalence; ii) impact on subsequent transmission to new naïve vertebrate hosts – expressed as reduction in infection of naïve mice (reduction in number of new malarial cases post-mosquito bite) and inhibition of subsequent parasitemia (day 10 post-bite) in mice that do become infected; iii) Effect size generated – by fitting the data achieved within this assay to a chain-binomial model we can assess the ability of DDD107498 to reduce R_0 (assuming 100% coverage). If R_0 is reduced to <1, transmission is unsustainable and elimination will occur. 95% CIs are

shown in brackets. Efficacy is calculated in comparison with no-drug controls. TB is transmission blocking



Extended Data Figure 7. ClustalWS alignment of eEF2 sequences from Human (*Hs*), Yeast (*Sc*) and *Plasmodium falciparum* (*Pf*) Alignment made using Jalview ClustalX default colouring.



Extended Data Figure 8. Fitness phenotypes of DDD107498-resistant parasite lines

Unmarked Dd2 and DDD107498-selected parasites with various levels of resistance were assessed for growth in a competition assay, relative to a Dd2-GFP reference line. **a.** Equal numbers of unmarked test lines were mixed with the Dd2-GFP reference, in triplicate wells, and the ratio of non-fluorescent and fluorescent cells assessed by flow cytometry over time. At day 0, all lines had a 1:1 ratio with the Dd2-GFP reference. Increased growth of the test line over the Dd2-GFP reference, which has a slower growth rate than unmarked WT Dd2, would result in an increased ratio of Test:Dd2-GFP. **b.** Growth assay of 4 different test lines: i) WT Dd2, ii) EF2-E134D, iii) EF2-L775F, and iv) EF2-Y186N, relative to Dd2-GFP. A faster growth rate of WT Dd2 (DDD107498 IC₅₀ 0.14 nM) relative to the fluorescent Dd2-GFP line is reflected in an increased ratio over time. The low-level resistant line EF2-E134D (IC₅₀ 5.8 nM) did not attain a WT growth rate, and the high-level resistant lines EF2-L775F (IC₅₀ 660 nM) and EF2-Y186N (3100 nM) were further impaired. Means ± s.d.; n=4 independent experiments each run in triplicate.

Extended Data Table 1
Pharmacokinetics and Rodent Efficacy of DDD107498

a. *In vivo* pharmacokinetic parameters in preclinical species (n=3, all species). **b.** Oral *in vivo* single dose efficacy of antimalarial drugs and DDD107498 in the murine *P. berghei* model.

a			
	Mouse	Rat	Dog
Intravenous	1 mg/kg	1 mg/kg	1 mg/kg
CI (ml/min/g)	12	18	30
V _{dss} (L/kg)	15	15	30
T _{1/2} (h)	16	10	13
Oral			
	3 mg/kg	5 mg/kg	3 mg/kg
C _{max} (ng/ml)	90	180	27
T _{max} (h)	1	4	4
T _{1/2} (h)	19	18	20
F%	74	84	46

b						
Compound	30 mg/kg		10 mg/kg		3 mg/kg	
	Activity %	Survival days	Activity %	Survival days	Activity %	Survival days
Chloroquine	§99.9	10	99.5	7	83	7
Mefloquine	§99.6	22	95	16	<40	7
Artemether	98	7	89	6	59	6
Dihydroartemisinin	99	7	97	6	61	7
Artesunate	§92	9	75	6	<40	6
DDD107498	99.1	23	99.0	14	99	9

Data are the means of n=3 for DDD107498 and n = 5 for the reference compounds.

§Data from Charman et al.³⁶.

Extended Data Table 2

Summary of resistance selection experiments with DDD107498

Strain	Pressure (nM)	Pressure (x IC ₅₀)	Inoculum* Number of positive cultures (day of recrudescence)						MIR	EC ₅₀ shift (inoculum) [†]
			10 ⁴	10 ⁵	10 ⁶	10 ⁷	10 ⁸	10 ⁹		
Dd2	1.25	2.7	ND [‡]	ND	2 (13, 41)	3 (13,13,15)	3 (13,13,16)	3 (29/29/29)	ND	2315 (10 ⁶)
										7 (10 ⁸)
										4810 (10 ⁶)
Dd2	1.26	27	0	0	0	3 (20,22,22)	ND	ND	10 ⁷	13 (10 ⁷)
Dd2	1.25	2.7	ND	0	1 (39)	ND	ND	ND	10 ⁶	5567 (10 ⁶)
7G8	1.25	3.1	ND	ND	0	3 (25, 25, 47)	1 (25)	3 (15,15,15)	10 ⁷	70 (10 ⁶)
										60 (10 ⁸)
										82 (10 ⁷)
3D7	1.5	3.3	ND	ND	0	2 (38, 38)	2 (28,28)	3 (20,20,20)	10 ⁷	19 (10 ⁶)
										99 (10 ⁸)
										14(10 ⁷)

* Number of positive cultures (n=3) and day of recrudescence for each inoculum.

[†] EC₅₀ fold change was determined on bulk cultures.[‡] Not determined. MIR is the Minimum Inoculum of Resistance.

Supplementary Material

Refer to Web version on PubMed Central for supplementary material.

Authors

Beatriz Baragaña¹, Irene Hallyburton¹, Marcus C. S. Lee², Neil R. Norcross¹, Raffaella Grimaldi¹, Thomas D. Otto³, William R. Proto³, Andrew M. Blagborough⁴, Stephan Meister⁵, Grennady Wirjanata⁶, Andrea Ruecker⁴, Leanna M. Upton⁴, Tara S. Abraham², Mariana J. Almeida², Anupam Pradhan⁷, Achim Porzelle¹, María Santos Martínez⁸, Judith M. Bolscher⁹, Andrew Woodland¹, Suzanne Norval¹, Fabio Zuccotto¹, John Thomas¹, Frederick Simeons¹, Laste Stojanovski¹, Maria Osuna-Cabello¹, Paddy M. Brock⁴, Tom S. Churcher⁴, Katarzyna A. Sala⁴, Sara E. Zakutansky⁴, María Belén Jiménez-Díaz⁸, Laura Maria Sanz⁸, Jennifer Riley¹, Rajshekhar Basak², Michael Campbell¹⁰, Vicky M. Avery¹¹, Robert W Sauerwein⁹, Koen J. Dechering⁹, Rintis Noviyanti¹², Brice Campo¹³, Julie A. Frearson¹, Iñigo Angulo-Barturen⁸, Santiago Ferrer-Bazaga⁸, Francisco Javier Gamo⁸, Paul G. Wyatt¹, Didier Leroy¹³, Peter Siegl¹³, Michael J. Delves⁴, Dennis E. Kyle⁷, Sergio Wittlin¹⁴, Jutta Marfurt⁶, Ric N. Price^{6,15}, Robert E. Sinden⁴, Elizabeth Winzeler⁵, Susan A. Charman¹⁰, Lidiya Bebrevska¹³, David W. Gray¹, Simon Campbell¹³, Alan H. Fairlamb¹, Paul Willis¹³, Julian C. Rayner³, David A. Fidock^{2,16}, Kevin D. Read¹, and Ian H. Gilbert¹

Affiliations

¹ Drug Discovery Unit, Division of Biological Chemistry and Drug Discovery, College of Life Sciences, University of Dundee, Dundee, DD1 5EH, UK. ² Department of Microbiology and Immunology, Columbia University College of Physicians and Surgeons, New York, NY 10032, USA. ³ Malaria Programme, Wellcome Trust Sanger Institute, Wellcome Trust Genome Campus, Cambridge CB10 1SA, UK. ⁴ Cell and Molecular Biology, Department of Life Sciences, Imperial College, London, SW7 2AZ, UK. ⁵ University of California, San Diego, School of Medicine, 9500 Gilman Drive 0760, La Jolla, CA 92093, USA. ⁶ Global Health and Tropical Medicine Division, Menzies School of Health Research, Charles Darwin University, Darwin, Northern Territory, Australia. ⁷ Department of Global Health, College of Public Health, University of South Florida, 3720 Spectrum Blvd, Suite 304, Tampa, FL 33612, USA. ⁸ GlaxoSmithKline, Tres Cantos Medicines Development Campus-Diseases of the Developing World, Severo Ochoa 2, Tres Cantos 28760, Madrid, Spain. ⁹ TropiQ Health Sciences, Geert Grooteplein 28, Huispost 268, 6525 GA Nijmegen, The Netherlands. ¹⁰ Centre for Drug Candidate Optimisation, Monash University, 381 Royal Parade, Parkville, Victoria 3052 Australia. ¹¹ Eskitis Institute, Brisbane Innovation Park, Nathan Campus, Griffith University, QLD, Australia 4111 ¹² Eijkman Institute for Molecular Biology, Jakarta, Indonesia. ¹³ Medicines for Malaria Venture, PO Box 1826, 20 route de Pre-Bois, 1215 Geneva 15, Switzerland. ¹⁴ Swiss Tropical and Public Health Institute, Socinstrasse 57, 4051 Basel, Switzerland. ¹⁵ Centre for Tropical Medicine and Global Health, Nuffield Department of Medicine, University of Oxford, UK ¹⁶ Division of Infectious Diseases,

Department of Medicine, Columbia University College of Physicians and Surgeons,
New York, NY 10032, USA

Acknowledgements

This work was supported by grants from Medicines for Malaria Venture, the Wellcome Trust (100476 (IHG, AHF), 091625 (RNP) and 098051 (JCR, WP, TDO)), the Bill and Melinda Gates Foundation (OPP1043501 (MD, RS)), the NIH (R01 AI103058 to EAW and DAF) and the European Union (EVIMalaR (TDO)). DDU infrastructure was supported by the European Regional Development Fund 2007-2013 and UK Research Partnership Investment Fund awards to Michael Ferguson, who we also thank for continued support. We would like to thank Prof Carol Sibley, University of Washington for helpful discussions. We acknowledge the East Scotland Blood Transfusion Service, Ninewells Hospital, Dundee for erythrocyte supply to Dundee. We thank L. D. Shultz and The Jackson Laboratory for providing access to nonobese diabetic scid IL2R γ c null mice through their collaboration with GSK Tres Cantos Medicines Development Campus. The following are acknowledged for technical assistance: all members of the DDU (Dundee), Matthew Berriman, Jolanda Kamber, Enny Kenangalem, Alexis LaCrué, Oliver Montagnat, Jeanne Rini Poespoprodjo, Mandy Sanders, Sibylle Sax, Christian Scheurer, Leily Trianty, Mark Tunnicliff (detailed in Supplementary Information).

References

1. WHO. World Malaria Report 2014. 2014 ISBN 978 992 974 156483 156480.
2. Ariey F, et al. A molecular marker of artemisinin-resistant *Plasmodium falciparum* malaria. *Nature*. 2014; 505:50–55. [PubMed: 24352242]
3. Alonso PL, et al. A research agenda for malaria eradication: Drugs. *PLoS Med*. 2011; 8:e1000402. [PubMed: 21311580]
4. Wells TNC, Gutteridge WE. *Neglected Diseases and Drug Discovery*. 2012:1–32. RSC.
5. Brenk R, et al. Lessons learnt from assembling screening libraries for drug discovery for neglected diseases. *ChemMedChem*. 2008; 3:435–444. [PubMed: 18064617]
6. Delves M, et al. The activities of current antimalarial drugs on the life cycle stages of *Plasmodium*: A comparative study with human and rodent parasites. *PLoS Med*. 2012; 9:e1001169. [PubMed: 22363211]
7. Russell B, et al. Determinants of in vitro drug susceptibility testing of *Plasmodium vivax*. *Antimicrob. Agents Chemother*. 2008; 52:1040–1045. [PubMed: 18180357]
8. Karyana M, et al. Malaria morbidity in Papua Indonesia, an area with multidrug resistant *Plasmodium vivax* and *Plasmodium falciparum*. *Malaria J*. 2008; 7:148.
9. Angulo-Barturen I, et al. A murine model of falciparum-malaria by *in vivo* selection of competent strains in non-myelodepleted mice engrafted with human erythrocytes. *PLoS One*. 2008; 3:e2252. [PubMed: 18493601]
10. Sanz LM, et al. *P. falciparum* in vitro killing rates allow to discriminate between different antimalarial mode-of-action. *PLoS One*. 2012; 7:e30949. [PubMed: 22383983]
11. Burrows JN, van Huijsduijnen RH, Mohrle JJ, Oeuvray C, Wells TN. Designing the next generation of medicines for malaria control and eradication. *Malar. J*. 2013; 12:187. [PubMed: 23742293]
12. Meister S, et al. Imaging of *Plasmodium* liver stages to drive next-generation antimalarial drug discovery. *Science*. 2011; 334:1372–1377. [PubMed: 22096101]
13. Adjalley SH, et al. Quantitative assessment of *Plasmodium falciparum* sexual development reveals potent transmission-blocking activity by methylene blue. *Proc. Natl. Acad. Sci. U S A*. 2011; 108:E1214–1223. [PubMed: 22042867]
14. Bousema T, Drakeley C. Epidemiology and infectivity of *Plasmodium falciparum* and *Plasmodium vivax* gametocytes in relation to malaria control and elimination. *Clin. Microbiol. Rev*. 2011; 24:377–410. [PubMed: 21482730]

15. Delves MJ, et al. Male and female *Plasmodium falciparum* mature gametocytes show different responses to antimalarial drugs. *Antimicrob. Agents Chemother.* 2013; 57:3268–3274. [PubMed: 23629698]
16. Delves MJ, et al. A high-throughput assay for the identification of malarial transmission-blocking drugs and vaccines. *Int. J. Parasitol.* 2012; 42:999–1006. [PubMed: 23023046]
17. Blagborough AM, et al. Transmission-blocking interventions eliminate malaria from laboratory populations. *Nat. Commun.* 2013; 4:1812. [PubMed: 23652000]
18. Upton LM, et al. Lead clinical and preclinical antimalarial drugs can significantly reduce sporozoite transmission to vertebrate populations. *Antimicrob. Agents Chemother.* 2015; 59:490–497. [PubMed: 25385107]
19. Janse CJ, et al. High efficiency transfection of *Plasmodium berghei* facilitates novel selection procedures. *Mol. Biochem. Parasitol.* 2006; 145:60–70. [PubMed: 16242190]
20. Flannery EL, Fidock DA, Winzeler EA. Using genetic methods to define the targets of compounds with antimalarial activity. *J. Med. Chem.* 2013; 56:7761–7771. [PubMed: 23927658]
21. Rottman M, et al. Spiroindolones, a potent compound class for the treatment of malaria. *Science.* 2010; 329:1175–1180. [PubMed: 20813948]
22. McNamara CW, et al. Targeting Plasmodium PI(4)K to eliminate malaria. *Nature.* 2013; 504:248–253. [PubMed: 24284631]
23. Miotto O, et al. Multiple populations of artemisinin-resistant *Plasmodium falciparum* in Cambodia. *Nat. Genet.* 2013; 45:648–655. [PubMed: 23624527]
24. Jorgensen R, Merrill AR, Andersen GR. The life and death of translation elongation factor 2. *Biochem. Soc. Trans.* 2006; 34:1–6. [PubMed: 16246167]
25. Justice MC, et al. Elongation factor 2 as a novel target for selective inhibition of fungal protein synthesis. *J. Biol. Chem.* 1998; 273:3148–3151. [PubMed: 9452424]
26. Capa L, Mendoza A, Lavandera JL, de las Heras FG, Garcia-Bustos JF. Translation elongation factor 2 is part of the target for a new family of antifungals. *Antimicrob. Agents Chemother.* 1998; 42:2694–2699. [PubMed: 9756779]
27. Shastry M, et al. Species-specific inhibition of fungal protein synthesis by sordarin: identification of a sordarin-specificity region in eukaryotic elongation factor 2. *Microbiology.* 2001; 147:383–390. [PubMed: 11158355]
28. Jorgensen R, et al. Two crystal structures demonstrate large conformational changes in the eukaryotic ribosomal translocase. *Nat. Struct. Biol.* 2003; 10:379–385. [PubMed: 12692531]
29. Nkrumah LJ, et al. Efficient site-specific integration in *Plasmodium falciparum* chromosomes mediated by mycobacteriophage Bxb1 integrase. *Nat. Methods.* 2006; 3:615–621. [PubMed: 16862136]
30. Biswas S, et al. Interaction of apicoplast-encoded elongation factor (EF) EF-Tu with nuclear-encoded EF-Ts mediates translation in the *Plasmodium falciparum* plastid. *Int. J. Parasitol.* 2011; 41:417–427. [PubMed: 21163263]
31. Cox G, et al. Ribosome clearance by FusB-type proteins mediates resistance to the antibiotic fusidic acid. *Proc. Natl. Acad. Sci. U S A.* 2012; 109:2102–2107. [PubMed: 22308410]
32. Ding XC, Ubben D, Wells TN. A framework for assessing the risk of resistance for anti-malarials in development. *Malar. J.* 2012; 11:292. [PubMed: 22913649]
33. Manske M, et al. Analysis of *Plasmodium falciparum* diversity in natural infections by deep sequencing. *Nature.* 2012; 487:375–379. [PubMed: 22722859]
34. Florens L, et al. A proteomic view of the *Plasmodium falciparum* life cycle. *Nature.* 2002; 419:520–526. [PubMed: 12368866]
35. Jimenez-Diaz MB, et al. Quantitative measurement of *Plasmodium*-infected erythrocytes in murine models of malaria by flow cytometry using bidimensional assessment of SYTO-16 fluorescence. *Cytometry. Part A : the journal of the International Society for Analytical Cytology.* 2009; 75:225–235. [PubMed: 18785271]
36. Charman SA, et al. Synthetic ozonide drug candidate OZ439 offers new hope for a single-dose cure of uncomplicated malaria. *Proc. Natl. Acad. Sci. U S A.* 2011; 108:4400–4405. [PubMed: 21300861]

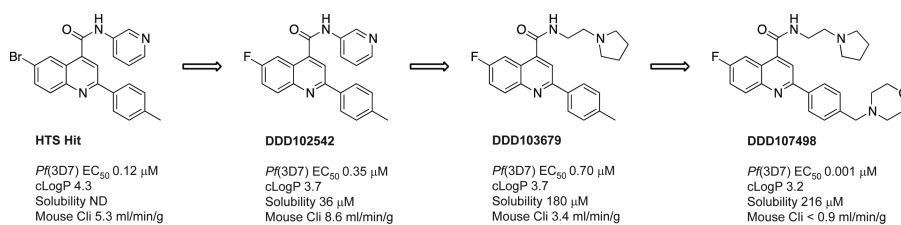


Figure 1. Chemical evolution of DDD107498 from the phenotypic hit

Cli = intrinsic clearance in mouse liver microsomes.

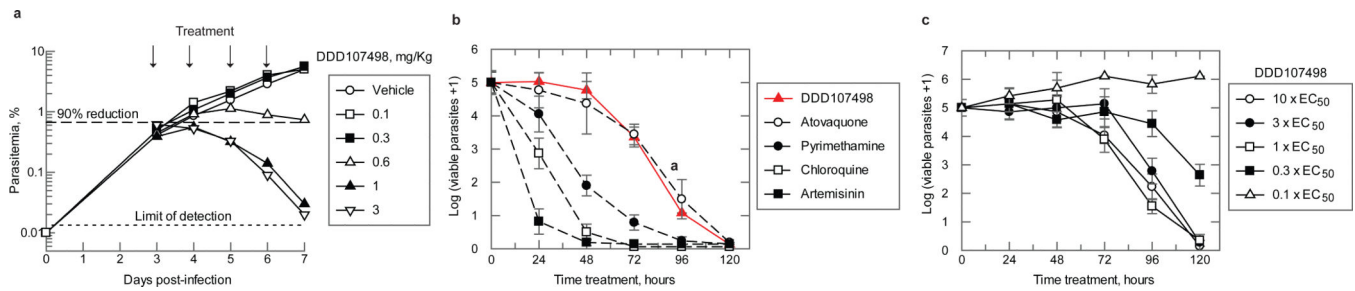


Figure 2. Efficacy studies and parasite killing rate

a. *In vivo* activity against *P. falciparum* in NOD-*scid* IL-2R_{null} mice. Six mice were used, each serially sampled. The variability of cytometry for repeated acquisitions of a sample is < 2-3 %. The percentage of parasitemia was calculated by acquiring a minimum number of 500 parasitized erythrocytes. An independent experiment with 3 further mice was performed to confirm the ED₉₀.

b. Determination of the *in vitro* killing rate of DDD107498. The *in vitro* PRR assay was used to determine onset of action and rate of killing as previously described¹⁰. *P. falciparum* was exposed to DDD107498 at a concentration corresponding to 10 × EC₅₀. The number of viable parasites at each time point was determined as described¹⁰. Four independent serial dilutions were done with each sample to correct for experimental variation and the error bars shown are the standard deviation. Previous results reported on standard antimalarials tested at 10 × EC₅₀ using the same conditions are shown for comparison¹⁰.

c. The *in vitro* PRR assay was used to determine the minimal concentration of compound needed for achieving maximal killing effects. Parasites were exposed to DDD107498 at concentrations of 0.1, 0.3, 1, 3 and 10 × EC₅₀ using conditions described above. Error bars shown are the standard deviation. Concentrations of DDD107498 1 × EC₅₀ are sufficient to produce maximal killing effects on treated parasites.

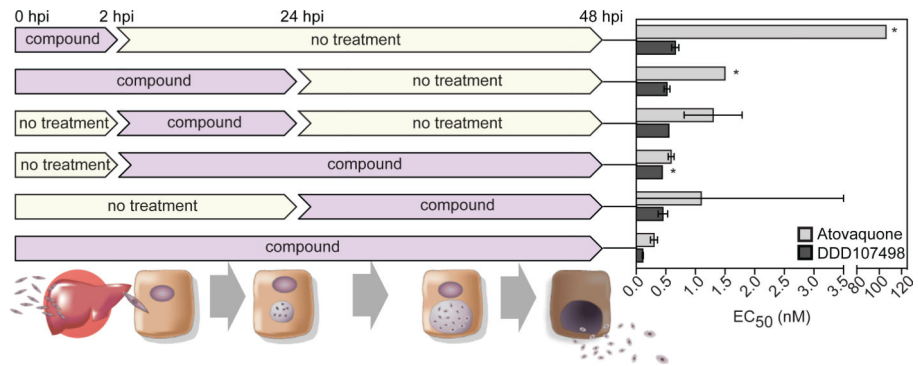


Figure 3. *In vitro* activity of DDD107498 against *P. berghei* liver stages
 hpi is hours post-infection. Each time point was the average of 4 technical replicates. 95% Confidence limits are shown. * more than one curve fitting possible.

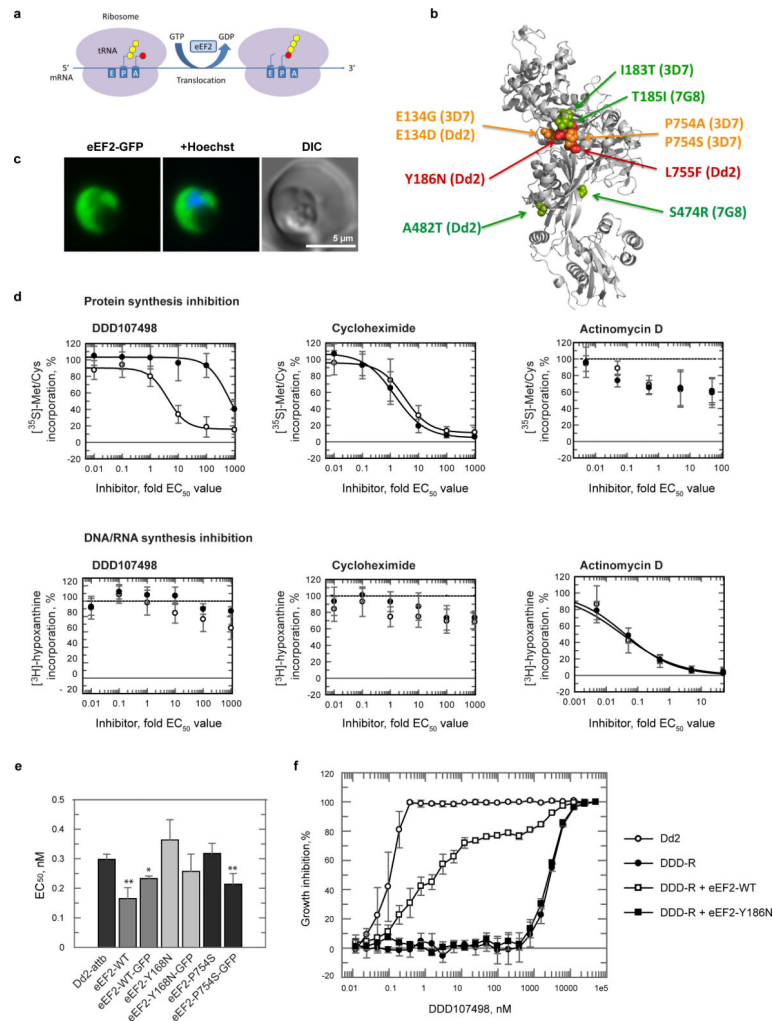


Figure 4. eEF2

- a. eEF2 promotes the GTP-dependent translocation of the ribosome along mRNA during protein synthesis.
- b. Homology model of *Plasmodium falciparum* eEF2. The mapped mutations from each strain are colour coded by EC₅₀ fold (red high, amber moderate, green low).
- c. Live cell imaging of *P. falciparum* expressing an extra copy of eEF2 (WT) fused to GFP. The image is representative of >50 parasites visualized on two independent occasions.
- d. Protein and DNA/RNA synthesis were evaluated by measuring the incorporation of [³⁵S]-labelled methionine and cysteine ([³⁵S]-Met/Cys) (upper panel) and [³H]-labelled hypoxanthine (lower panel) into asynchronous 3D7 wild-type (○) and 3D7 DDD107498-resistant line (eEF2-E134A/P754A) (●) after 40 min incubation with DDD107498, cycloheximide or actinomycin D. Radiolabeled incorporation, measured as cpm, was normalised as % of incorporation against inhibitor concentration (means ± s.d.; n=3 independent experiments each run in duplicate).
- e. The EC₅₀ values for transfectants against DDD107498 (means ± s.d.; n=4-7 independent experiments, each run in duplicate). Statistical significance was determined by the Mann-Whitney U test: *P<0.05; **P<0.01.

f. DDD107498-resistant line (eEF2-Y186N) transfected episomally with plasmids expressing either WT-eEF2 or eEF2-Y186N (means \pm s.d.; n=3 independent experiments each run in duplicate).

Author Manuscript

Author Manuscript

Author Manuscript

Author Manuscript